Published for SISSA by Springer

Received: February 10, 2023
Revised: June 17, 2023
Accepted: June 23, 2023
Published: July 19, 2023

Can leptonic mixing matrix have a Wolfenstein form?

Ankur Panchal,[a,b] **G. Rajasekaran**[c,d,1] **and Rahul Srivastava**[a,2]

[a] *Department of Physics, Indian Institute of Science Education and Research - Bhopal, Bhopal Bypass Road, Bhauri, Bhopal 462066, India*
[b] *Indian Institute of Science Education and Research - Pune, Dr. Homi Bhabha Road, Pashan, Pune, India*
[c] *The Institute of Mathematical Sciences, Chennai 600 113, India*
[d] *Chennai Mathematical Institute, Siruseri 603 103, India*

E-mail: panchal21@iiserb.ac.in, graj@imsc.res.in, rahul@iiserb.ac.in

Abstract: We analyze the possibility of the leptonic mixing matrix having a Wolfenstein form at the Grand Unified Theory scale. The renormalization group evolution of masses and mixing angles from the high scale to electroweak scale, in certain new physics scenarios, can significantly alter the form of the leptonic mixing matrix. In the past it was shown that such significant enhancement implies that the leptonic mixing matrix at high scale can be the same or similar in structure to the quark one. We thoroughly analyze this hypothesis in the light of the latest neutrino oscillation data as well as other constraints such as those coming from neutrinoless double beta decay. We show that such an ansatz, at least within the context of minimal supersymmetric models, is no longer compatible with the latest experimental data.

Keywords: Neutrino Mixing, Theories of Flavour

ArXiv ePrint: 2302.03878

[1] Deceased.
[2] Corresponding author.

https://doi.org/10.1007/JHEP07(2023)151

JHEP07(2023)151

Contents

1 Introduction

The Standard Model (SM) of particle physics has been an incredibly successful theory. Discovery of the 125-GeV scalar, if it is confirmed to be the SM Higgs boson, will complete the SM [1, 2]. However, in spite of its astounding success we now know that SM cannot be the complete theory of nature. The discovery of neutrino oscillations was one of the conclusive proofs for the shortcoming of the SM [3, 4]. Ever since the discovery of neutrino oscillations our understanding of the neutrino oscillation parameters and hence in turn that of the leptonic mixing matrix is improving. The precision in measurement of certain mixing parameters has dramatically improved over the last decade [5–7]. This implies that neutrino physics is now entering the era of precision physics where the experimental data, in particular from neutrino oscillation experiments, can be used to rule out new physics models in a much more powerful way. In this work we confront one of the popular theoretical proposals, namely the possibility of leptonic mixing matrix having a Wolfenstein form at some high energy scale.

In its original form the ansatz hypothesized a "High Scale Mixing Unification" (HSMU) between the lepton and quark mixing matrices [8]. Here the unification of the two mixing matrices was hypothesized to happen at some high scale typically chosen to be the scale of the Grand Unified Theories (GUTs). The Renormalization - Group (RG) evolution of the leptonic mixing angles and masses can then lead to the values of neutrino oscillation parameters within their experimental 3-σ range. One of the key prediction of the HSMU hypothesis was the prediction of a small yet non-zero value of θ_{13} leptonic mixing angle [8–15]. This was due to the fact that $\theta_{13} = 0$ is not a fixed point of the RG flow. Rather the RG evolution of the mixing angles from the high scale naturally leads to a small θ_{13}, a fact later observed in experimental measurements [5–7]. After the experimental measurement of θ_{13} angle, the HSMU hypothesis was revisited for both Dirac and Majorana neutrinos and it was shown that indeed HSMU can be a good candidate proposal for understanding of the neutrino mixing and oscillation phenomenon consistent with the experimental data of that time [12, 13]. The scale of high energy unification as well as dependence on other parameters was also analyzed in these later works showing that the scale of unification does not need to be necessarily the GUT scale. Still later works expanded the idea further looking at the possibility whether the leptonic mixing matrix has a "Wolfenstein form" with hierarchical values of mixing angles at high scale, irrespective of whether or not they are exactly same as quark mixing angles [16–19].

Overall, HSMU and its Wolfenstein form generalization have been shown to be consistent with successive sets of experimental data for increasingly precise determination of neutrino oscillation parameters over the past decade. However, as neutrino physics in entering the era of precision measurements, in this work we revisit it again to see if it still remains a viable possibility. The work-flow is presented in the rest of the paper in the following manner. Section 2 discusses the general framework of HSMU and RG evolution of neutrino oscillation parameters. Then in sections 3 and 4 we show our results of HSMU for Dirac and Majorana neutrinos. We find that the current oscillation data combined with other experimental constraints imply that HSMU ansatz is in severe tension with experiments. Further in section 5 we test whether or not the threshold corrections improve the negative results for HSMU ansatz. The next section 6 expands this unification hypothesis into Wolfenstein ansatz by introducing new free parameters. And finally we see conclusions from all the result's interpretations, section 7.

2 High Scale Mixing Unification Hypothesis

We start with a general discussion of the HSMU hypothesis and the essential ingredients needed to have a large change in values of leptonic mixing angles over the course of RG evolution from high to low energy scale.

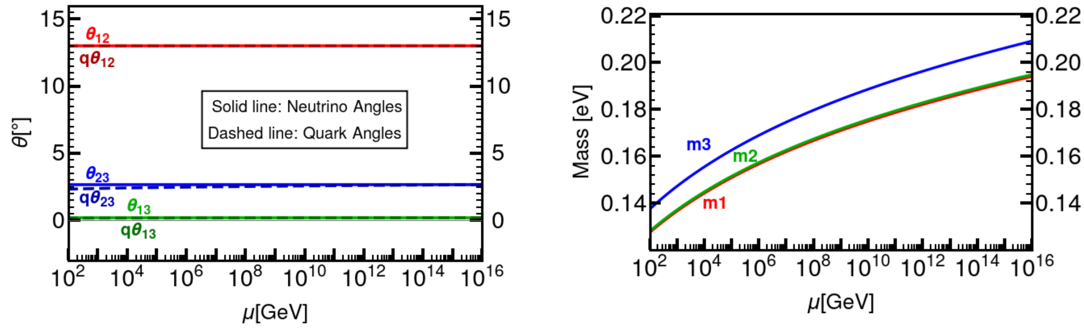

(a) Neutrino and quark mixing angles in SM.

(b) Neutrino masses in SM.

Figure 1. RG running of neutrino mixing angles and masses in SM from HSMU scale (taken as GUT scale) to low energy scale.

2.1 General framework of HSMU

Since HSMU assumes that at a high scale, usually taken as GUT scale, the quark and leptonic mixing matrices are one and same, this immediately implies that in order for HSMU to be consistent with neutrino oscillation data, a large change in neutrino mixing angles is needed. Unfortunately this cannot be achieved within SM extended by effective Weinberg operator[1] or it's simple Ultra-Violet (UV) completions such as Type-I seesaw. In figure 1 we show the RG evolution of the mixing angles of quarks and leptons (left panel) and Majorana neutrino masses (right panel) from the HSMU scale (take as GUT scale) to low scale within Type-I seesaw. As clear from figure 1, within SM + Type-I seesaw the neutrino mixing angles get enhanced by a negligible amount and hence HSMU hypothesis is completely inconsistent with neutrino oscillation data given in table 2.

The situation changes dramatically if there is beyond Standard Model (BSM) new physics at an intermediate scale such as a low scale SuperSymmetry (SUSY) at TeV scale. In figure 2 we show the RG evolution of neutrino and quark mixing angles (left panel) and the neutrino masses (right panel) with in Minimal SuperSymmetric Model (MSSM) from HSMU scale to SUSY breaking scale (taken as two TeV) followed by RG evolution in SM from SUSY breaking scale to low scale. As can be seen from figure 2, in this case a significant enhancement can be achieved during the MSSM part of RG evolution[2] provided we take large values of $\tan\beta$ and the neutrino masses at HSMU scale are normal ordered (N.O.) and quasi-degenerate [8–15]. In this work we will follow the previous works and throughout the work we will use MSSM as the intermediate theory with the SUSY breaking scale being two TeV. Moreover, we will always take $\tan\beta = 55$ and the unification scale will always be taken as the GUT scale (2×10^{16} GeV). The dependence and effect on our analysis due to change in HSMU scale, SUSY breaking scale and $\tan\beta$ were analyzed in

[1]RG evolution including Weinberg operator as effective operator can be done only if its UV cutoff scale is equal to or higher than the HSMU scale.

[2]Note that since SUSY is typically broken only softly, for RG evolution the details of SUSY breaking are irrelevant. However, in later section we will indeed discuss the leading SUSY threshold corrections and their impact on our analysis.

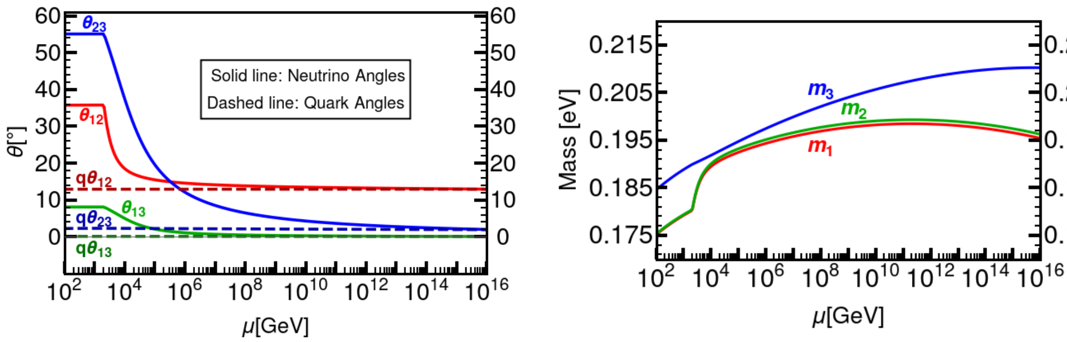

(a) Neutrino and quark mixing angles in MSSM.

(b) Neutrino masses in MSSM.

Figure 2. RG running of neutrino mixing angles and masses in SM and MSSM from HSMU scale (taken as GUT scale) to low energy scale. The SUSY breaking scale is taken to be two TeV.

Oscillation parameters	1-σ range	Best fit values
θ_{q12}	12.96° - 13.04°	13.00°
θ_{q13}	0.20° - 0.22°	0.21°
θ_{q23}	2.35° - 2.45°	2.40°
δ_q	63.99°-67.09°	65.55°

Table 1. Low scale Quark oscillation parameters data [20] δ_q is CP violation phase of quarks.

detail for Majorana neutrinos in ref. [13] and for Dirac neutrinos in ref. [12]. We will not repeat this analysis here as changing these scales will only increase the tension between the HSMU predictions and current experimental data.

Finally, before going to the sub-cases we must point out that the RG evolution of mixing angles and mass-squared differences are correlated with each other. This is because at high scale we only have three free parameters namely the "high scale masses" of the neutrinos using which we have to obtain five neutrino oscillation parameters within their 3-σ range at low scale. Furthermore, the RG equations governing the evolution of the mixing parameters are coupled partial differential equations and hence RG evolution of one parameter can strongly effect the RG evolution of the other parameters. As we will see, this means that the values of these parameters at low scale show strong correlations with each other and obtaining all the mixing parameters at low scale within their 3-σ ranges is non-trivial.

2.2 Computational implementation

Computationally, the implementation of HSMU can be looked at as a two-step process. First stage involves RG evolution of known values of CKM parameters (see table 1) from the low scale which we take as the mass scale of Z boson (M_Z), to the unification scale which is taken to be the GUT scale. While evolving from M_Z scale, we need to provide all known values of Gauge couplings, Yukawa couplings, CP violation phase (δ_q) and low scale quark mixing angles at low scale listed in appendix A. Below SUSY breaking scale SM RG

JHEP07(2023)151

Oscillation parameters	3-σ range	Best fit values
θ_{12}	31.37° - 37.41°	34.33°
θ_{13}	8.13° - 8.92°	8.53°
θ_{23}	41.21° - 51.35°	49.26°
Δm^2_{atm} ($10^{-3}eV^2$)	2.47-2.63	2.55
Δm^2_{sol} ($10^{-5}eV^2$)	6.94-8.14	7.50

Table 2. Global fit ranges for the neutrino oscillation parameters taking normal mass ordering (N.O.) of the neutrinos [28].

equations govern the evolution and above SUSY breaking scale the same is done by MSSM RG equations [21–27].

Now, according to HSMU hypothesis the high scale quark mixing angles are equated with high scale neutrino mixing angles.[3] To evaluate all the neutrino parameters at M_Z scale, we will also need neutrino masses at GUT scale. These are the free parameters of HSMU. With neutrino mixing angles equal to be those of quarks and masses taken as free parameters at the GUT scale, a top-down RG evolution is performed to obtain neutrino oscillation parameters at M_Z scale. We then check the compatibility of the so obtained neutrino oscillation parameters at low scale with the current global fit data listed in table 2.

In case of Majorana mass generation, an effective dimension-5 operator is added in the Lagrangian below seesaw scale. Above the seesaw scale, it's UV-completed using type-I seesaw mechanism. All right handed neutrinos added are integrated out below the seesaw scale. During implementation of the RG equations, we have ensured to use the appropriate RG equations above and below the SUSY cutoff scale as well as to correctly integrate out the right handed neutrinos for RG evolution below their mass threshold. All the RG runnings in this work are performed with the help of the Mathematica based package REAP [26].

3 Dirac case

We begin our detailed analysis starting with the case of Dirac neutrinos. If neutrinos are Dirac fermions then by definition, one must add three right handed neutrinos, one for each generation, to the SM particle content. The simplest model for mass generation for Dirac neutrinos is through Higgs mechanism where the smallness of neutrino mass is due to small Yukawa couplings.[4] As mentioned before, for HSMU one needs SUSY at the TeV scale which in its simplest form can be implemented by embedding SM in MSSM with three additional superfields embedding the right handed neutrinos. The Lagrangians before and after SUSY breaking scale are given by

Below SUSY breaking scale:

$$\mathcal{L} = \mathcal{L}_{SM} + \mathcal{L}_{\nu_R} = \mathcal{L}_{SM} - Y^{ij}_{\nu}\bar{L}^i\tilde{H}\nu^j_R + h.c. \tag{3.1}$$

[3]We will analyze both cases where the CP phase is also equated and the case where it is taken zero. Majorana phases when taken non-zero are treated as free parameters.

[4]In literature there exist various other mass generation mechanisms for Dirac neutrinos, interested readers can see refs. [29–38] for some of the recent works and ref. [39] for a review.

JHEP07(2023)151

Above SUSY breaking scale:

$$\mathcal{L} = \mathcal{L}_{\text{MSSM}} + \mathcal{L}_{\nu_{\text{R}}} = \mathcal{L}_{\text{MSSM}} - \mathbb{Y}_{\nu}^{ij} \bar{\mathbb{L}}^i \mathbb{H}_2 \mathbb{N}_R^j + h.c, \tag{3.2}$$

where i, j, k are flavor indices, Y_ν is the Yukawa matrix for the neutrinos, $\nu_{\text{R}}^{\text{i}}$ is a right handed neutrino of flavor i and $\mathbb{L}, \mathbb{H}_2, \mathbb{N}$ are the corresponding fields in the MSSM. Also, we denote the two $\text{SU}(2)_L$ scalars doublets in MSSM by $\mathbb{H}_1, \mathbb{H}_2$ with their $\text{U}(1)_Y$ charges given by $\mathbb{H}_1 \sim +1/2, \mathbb{H}_2 \sim -1/2$ whereas the $\text{U}(1)_Y$ charge of the lepton doublet is $\mathbb{L} \sim -1/2$. The RG equations for the evolution of neutrino masses and mixing parameters for this case can be found in [27].

The implementation of HSMU ansatz in this case follows the general strategy discussed in previous section. We start with the known values of the quark masses, mixing parameters, gauge couplings etc at the low scale (M_Z). We use the SM RG equations for the evolution up to SUSY breaking scale (2 TeV) and then use the MSSM RG equations up to the high scale (GUT scale). At the GUT scale we fix the leptonic mixing angles and depending on the case (see discussion below) the CP phase also, to be equal to the quark ones. The neutrino masses at GUT scale are taken as N.O. and are treated as free parameters. We then do RG running back to the low scale to obtain the RG evolved values of the neutrino oscillation parameters and compare with the global fit data [28].

In this case, we consider two sub-cases: one when there is no CP violation in the leptonic sector i.e the CP phase $\delta = 0$ and the other when there is CP violation in the leptonic sector as well i.e. $\delta \neq 0$. In the second case following HSMU ansatz, at high scale we take $\delta = \delta_q$. We analyze both cases one by one.

3.1 CP conserving $\delta = 0$ case

The experimental situation regarding CP violation in leptonic sector is still not clear. Thus there is possibility that there is no CP violation in leptonic sector, this implies that the CP phase $\delta = 0$. The CP phase being zero is a fixed point in RG evolution which means that if $\delta = 0$ at high scale it will remain zero at the low scale as well. Thus, for the case of CP conservation in leptonic sector, one must take $\delta = 0$ at the HSMU scale.

As mentioned before, within HSMU hypothesis the RG evolution of neutrino oscillation parameters are correlated. In figure 3 we show the obtained values of θ_{23} and θ_{13} at low scale for benchmark values of θ_{12} angle. The shaded region (light red) corresponds to values of θ_{23} and θ_{13} outside their 3-σ range given in table 2. The white rectangular region corresponds to allowed values of both θ_{23} and θ_{13} simultaneously. For the correlation line passing through the allowed region, θ_{12} is 14.17° which is an outside 3-σ low scale value for θ_{12}. Thus this line can be discarded as we can not have the low scale values of all three angles within their 3-σ ranges. When θ_{12} is varied the linear correlation function moves with respect to the allowed (white) region. If θ_{12} is increased the line moves to the top-left corner of the allowed region, indicating that for those values of θ_{12} we can not have θ_{23} and θ_{13} within their 3-σ ranges. We can see that for the entire allowed range of θ_{12} values, the corresponding blue band is completely outside the allowed region for θ_{23} and θ_{13}, which tells us that we cannot have a suitable case where all of the mixing angles lie within their allowed ranges. This happens because RG equations are monotonous functions of θ_{12} and therefore

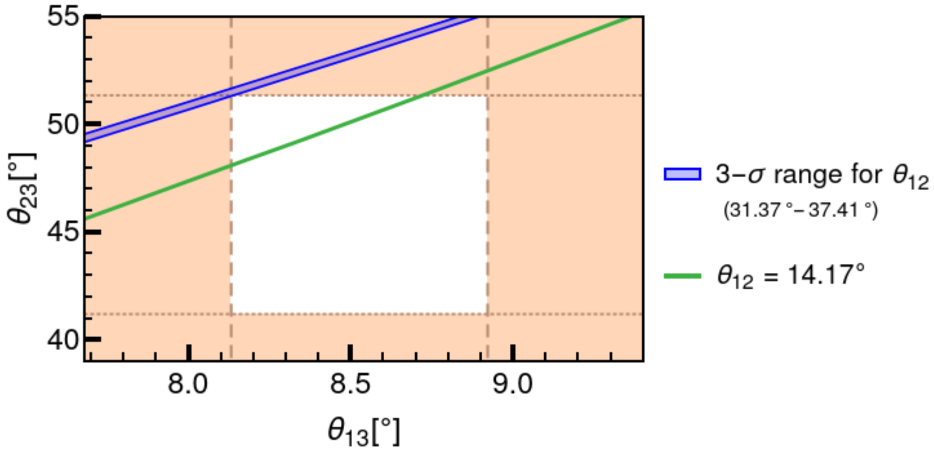

Figure 3. θ_{23} vs θ_{13} with $\delta = 0°$. The correlation is a straight line. Different straight lines would correspond to different θ_{12}. The light red region represents rejected values of θ_{23} and θ_{13} which are out of their 3-σ ranges. The blue band represents the contour lines for all allowed θ_{12} values within its 3-σ range.

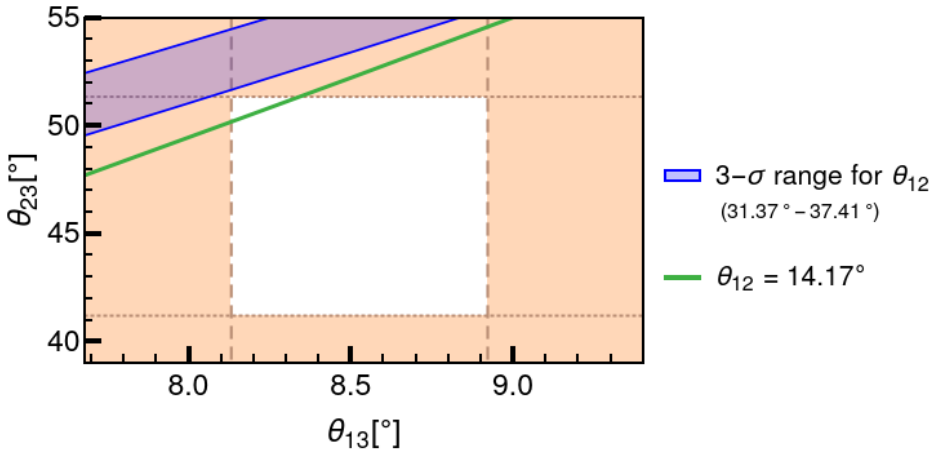

Figure 4. θ_{23} vs θ_{13} with $\delta \neq 0°$. At GUT scale the value of δ is set equal to δ_q at that scale. The shaded regions carry the same meaning as that in the previous figure.

increment in the value of θ_{12} moves the θ_{12} contour away from the allowed region and thus the blue band which corresponds to higher values of θ_{12} lies outside the white region.

3.2 CP violating $\delta = \delta_q$ case

In this case we take δ at high scale to be equal to quark sector CP violating phase at high scale i.e. $\delta = \delta_q$ at the HSMU scale. Running down from GUT scale to M_Z scale, we still can't have all three angles inside their 3-σ ranges, as can be seen from figure 4. The result remains the same as in CP conserving case. Allowed values of θ_{12} corresponding to the blue band, lie completely outside the allowed region of the θ_{23}–θ_{13} plane.

Thus, for the case of Dirac neutrinos neither CP conserving nor CP violating cases allow us to have all mixing angles within their 3-σ range. Since mixing angles don't agree

JHEP07(2023)151

with the experimental values for Dirac case, it is redundant to check the same for mass squared differences. Hence, we can conclude that although HSMU for Dirac neutrinos was a valid possibility in the past [12], the current more stringent data rules it out as a viable possibility.

4 Majorana case

In this case we consider neutrinos to be Majorana particles whose mass is generated through Type-I seesaw mechanism. Current limits on neutrino mass [40, 41] imply that if all Yukawas are taken within their perturbative range then the Type-I seesaw scale has to be smaller than the GUT scale. Throughout this work we will take the seesaw scale to be $\sim 10^{12}$ GeV so that the neutrino Yukawa couplings remain perturbative across the entire range of RG running. In this case there are several scales and the Lagrangian used for RG running at each scale is shown in (4.1).

$$\begin{aligned}
&\text{Below SUSY breaking scale:}\\
&\mathcal{L}=\mathcal{L}_{\text{SM}}+\mathcal{L}_5\\
&\text{SUSY up to seesaw scale:}\\
&\mathcal{L}=\mathcal{L}_{\text{MSSM}}+\mathcal{L}_5\\
&\text{Seesaw to HSMU scale:}\\
&\mathcal{L}=\mathcal{L}_{\text{MSSM}}+\mathcal{L}_{\text{seesaw}}=\mathcal{L}_{\text{MSSM}}-\mathbb{Y}_\nu^{ij}\bar{\mathbb{L}}^i\mathbb{H}_2\mathbb{N}_R^i-\frac{1}{2}\mathbb{M}^{ij}(\bar{\mathbb{N}}^c)^j\mathbb{N}^j+\text{h.c.}
\end{aligned} \tag{4.1}$$

where $\mathbb{M}$ represents the Majorana mass matrix, $\mathbb{Y}$ is the Yukawa matrix and rest of the notation remains same as in (3.2). Furthermore, in (4.1), below seesaw scale, we have added the dimension five Weinberg operator ($\mathcal{L}_5$) obtained from integrating out the right handed neutrinos [42]. In its SUSY version it is given by

$$\mathcal{L}_5=-\frac{\kappa^{ij}}{\Lambda}(\bar{\mathbb{L}}^c)^i\mathbb{H}_2^\dagger\,\mathbb{L}^j\mathbb{H}_2^\dagger \tag{4.2}$$

where Λ is the cutoff scale for the effective operator which in our case is the seesaw scale and κ^{ij} is the effective coupling. After SUSY breaking the $\mathcal{L}_5$ becomes the canonical Weinberg operator added to the SM Lagrangian [42].

At the HSMU scale, apart from the masses of neutrinos we now have three additional free parameters, namely the three phases, the usual δ CP as well as the two Majorana phases φ_1 and φ_2. Here again we have to consider two sub-cases- one when Majorana phases are zero and the other when they are non-zero. For simplicity, we are fixing δ to be equal to δ_q at high scale. We have checked and verified that no CP violation ($\delta=0$) in Majorana case also leads to similar qualitative results as that of the case of $\delta=\delta_q$ and $\varphi_1=\varphi_2=0$. Therefore, in order to avoid unnecessary repetition, we will not present it separately.

Before looking at the sub-cases we should point out that for Majorana neutrinos one also has an additional constraint coming from the experimental searches of neutrinoless double beta decay ($0\nu\beta\beta$). The $0\nu\beta\beta$ experiments provide constraints on a particular

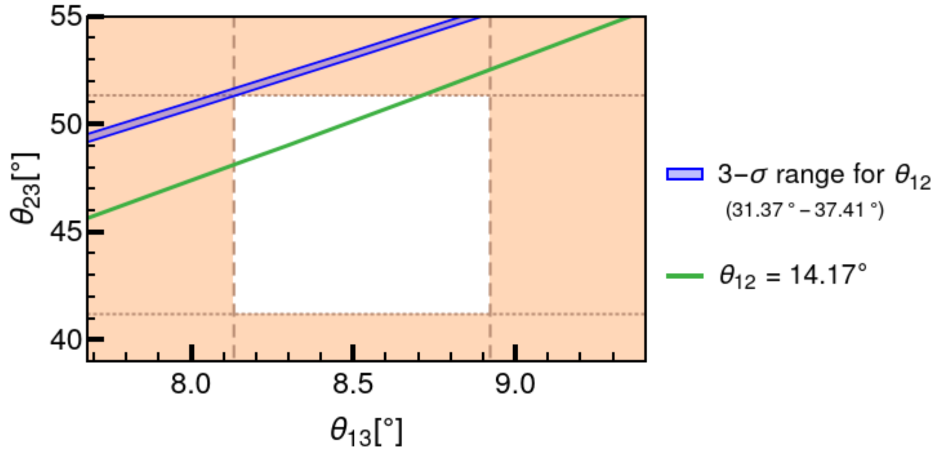

Figure 5. θ_{23} vs θ_{13} with $\varphi_1 = \varphi_2 = 0°$. The shaded regions carry the same meaning as that in the Dirac cases.

combination of neutrino masses and mixing parameters called the effective Majorana mass ($\mathrm{m}_{\beta\beta}$) which is given as

$$\mathrm{m}_{\beta\beta} = |c_{12}^2 c_{13}^2 m_1 + s_{12}^2 c_{13}^2 m_2 e^{i\varphi_1} + s_{13}^2 m_3 e^{i\varphi_2}| \tag{4.3}$$

where $\mathrm{c_{ij}} = \cos\theta_{\mathrm{ij}}$ and $\mathrm{s_{ij}} = \sin\theta_{\mathrm{ij}}$ denote the sine and cosine of the mixing angles.

The decay rate of $0\nu\beta\beta$ process $\Gamma \propto |m_{\beta\beta}|^2$. The most stringent upper bound range on $\mathrm{m}_{\beta\beta}$ is set by KamLAND-Zen experiment and its value ranges from 0.065 eV to 0.165 eV [43] depending on the choice of the nuclear matrix elements. In this paper we will use the conservative upper bound, i.e., we will demand that the low scale value of $\mathrm{m}_{\beta\beta} < 0.165$ eV.

4.1 Majorana phases, $\varphi_1 = \varphi_2 = 0°$

This case as well as the case of no leptonic CP violation are both qualitatively similar to Dirac cases of no leptonic CP violation and $\delta = \delta_q$, respectively. Like the Dirac case here again we first look at the correlated evolution of the mixing angles at the low scale. In figure 5 we show the correlation between low scale value of θ_{23} and θ_{13} mixing angles for benchmark choices of the θ_{12} angle. Just like the Dirac case, the three mixing angles cannot be simultaneously brought within their current 3-σ range. Since all three angles couldn't be brought into their 3-σ ranges, there is no reason to look into mass squared differences or $\mathrm{m}_{\beta\beta}$'s experimental constraints. To conclude, this case is also ruled out by the current experimental data.

4.2 Non-zero Majorana phases, $\varphi_1 \neq 0, \varphi_2 \neq 0$

In this case, apart from the neutrino masses at HSMU scale, we have two more free parameters namely the two Majorana phases, φ_1, φ_2 which cannot be constrained by the HSMU hypothesis. Non-zero values of the Majorana phases at HSMU scale strongly influence the RG evolution of the neutrino oscillation parameters. In fact, contrary to the previous cases here by appropriate choices of the two Majorana phases, one can indeed

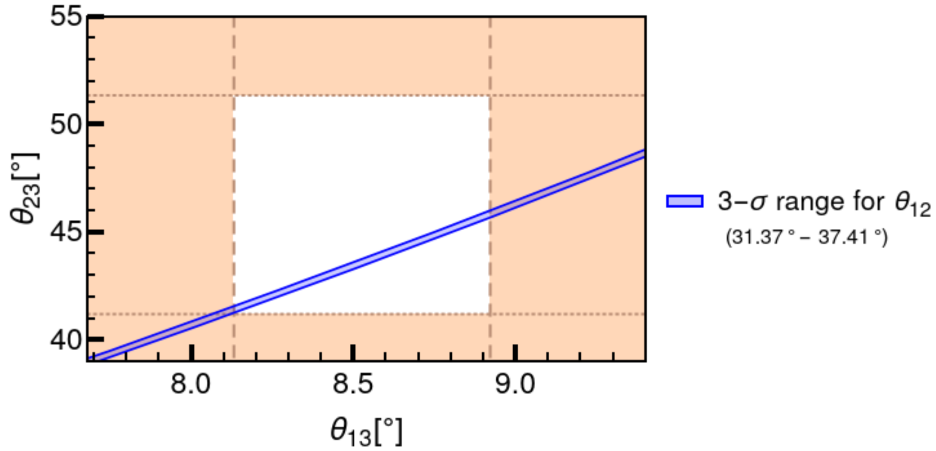

Figure 6. θ_{23} vs θ_{13} with $\varphi_1 = 120°$, $\varphi_2 = 30°$. The shaded regions carry the same meaning as that in the previous correlation plots.

simultaneously bring all the three mixing angles inside their 3-σ ranges. In figure 6 we show the correlation between θ_{23} and θ_{13} for the allowed range of θ_{12}, shown by the blue band, and for benchmark choices of the Majorana phases φ_1, φ_2.

Therefore this case needs closer inspection to see if there exist values of the Majorana phases for which the mass squared differences (Δm^2_{atm} and Δm^2_{sol}) can also be brought within their 3-σ range. In addition we also need to check if the experimental upper allowed limit of $m_{\beta\beta}$ is also respected. Thus one should check for all possible combinations of values of φ_1, φ_2. This is computationally very challenging. Fortunately, the dependence of the RG evolution of the mixing parameters on the Majorana phases is not completely arbitrary. Thus, instead of scanning through randomly generated values of all possible combinations of φ_1, φ_2 for the whole [0,2π] range of both phases, we manually choose some discrete benchmark values of them which clearly show the RG evolution pattern. To this end we fix one φ and record the effect of other φ on the low scale mixing angles as well as on Δm^2_{atm} & Δm^2_{sol} as we discuss now.

4.2.1 Effect of φ_1, φ_2 on Δm^2_{atm}, Δm^2_{sol}, $m_{\beta\beta}$ and $m_{lightest}$

The Majorana phases and neutrino masses are the only free parameters at the HSMU scale and their choices play a critical role in RG evolution of the neutrino oscillation parameters. At low scale, apart from the mixing angles one has to ensure that the mass squared differences Δm^2_{atm}, Δm^2_{sol} remain in their 3-σ range and $m_{\beta\beta}$ remains below its upper limit. It can be insightful to understand the extent by which we can bringing Δm^2_{atm}, Δm^2_{sol} and $m_{\beta\beta}$ in their allowed ranges. This can be analyzed by plotting them against one of the masses at the low scale. We choose the lightest neutrino mass ($m_{lightest} = m_1$) for the same. Figure 7 shows the trend of Δm^2_{atm}, Δm^2_{sol} and $m_{\beta\beta}$ plotted against $m_{lightest}$ with respect to the variations of φ_1, φ_2.

In figure 7 the solid lines represent Δm^2_{atm} or Δm^2_{sol} and dotted lines represent $m_{\beta\beta}$. The white bands in the plots show the 3-σ range of the mass squared differences. Furthermore,

JHEP07(2023)151

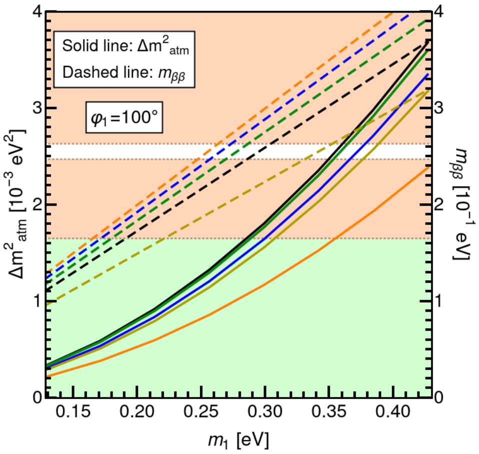

(a) Δm^2_{atm} vs $m_{lightest}$ for $\varphi_1 = 100°$.

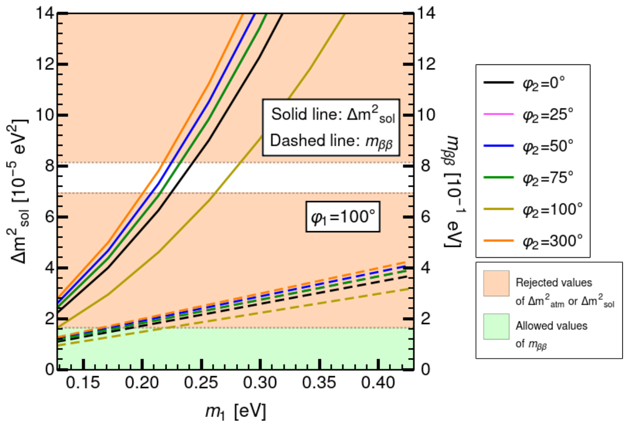

(b) Δm^2_{sol} vs $m_{lightest}$ for $\varphi_1 = 100°$.

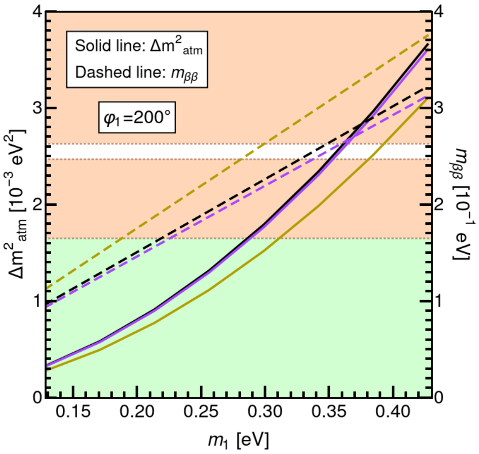

(c) Δm^2_{atm} vs $m_{lightest}$ for $\varphi_1 = 200°$.

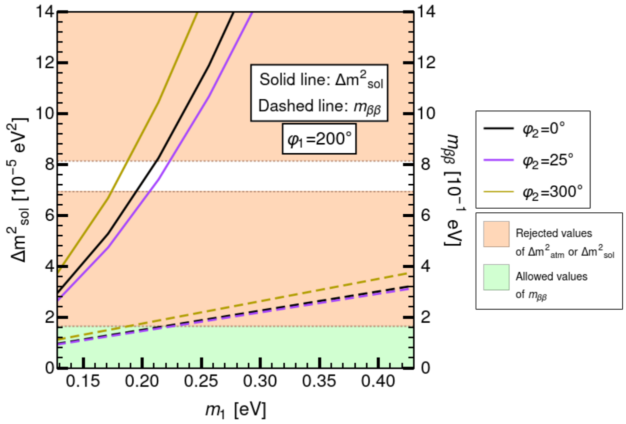

(d) Δm^2_{sol} vs $m_{lightest}$ for $\varphi_1 = 200°$.

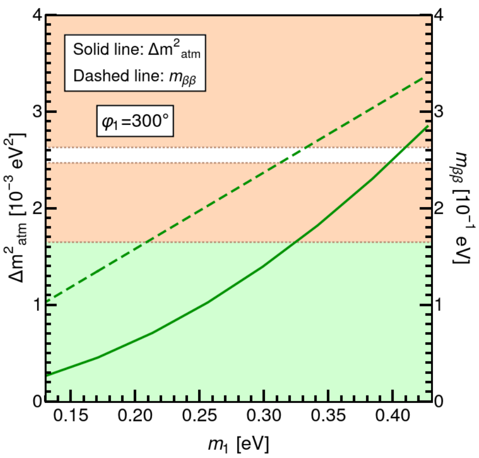

(e) Δm^2_{atm} vs $m_{lightest}$ for $\varphi_1 = 300°$.

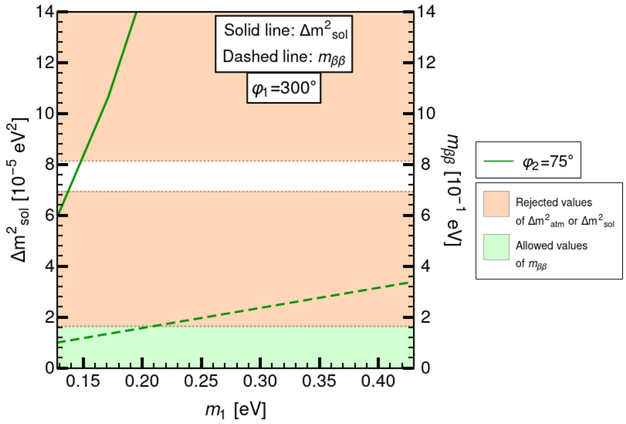

(f) Δm^2_{sol} vs $m_{lightest}$ for $\varphi_1 = 300°$.

Figure 7. The correlated evolution of Δm^2_{atm} (left panels) and Δm^2_{sol} (right panels) with respect to $m_{lightest}$ for different benchmark values of the Majorana phases φ_1, φ_2. Also plotted are the values of $m_{\beta\beta}$ with respect to $m_{lightest}$. Solid lines represent Δm^2_{atm} or Δm^2_{sol} and dotted lines represent $m_{\beta\beta}$. The white bands in the plots show the 3-σ range of the mass squared differences. Furthermore, in all the plots we have kept the three mixing angles always inside their 3-σ range. See text for more details.

in all the plots we have kept the three mixing angles always inside their 3-σ range. In the various panels of figure 7 we can notice the region on $m_{lightest}$ axis where the $m_{\beta\beta}$ dashed lines are below their upper bound. The solid lines for those $m_{\beta\beta}$ values can be inside the white region or outside the white region. Comparing graphs for Δm^2_{sol} and Δm^2_{atm} side by side one can estimate whether, for a particular set of Majorana phases or for a particular value of $m_{lightest}$, whether Δm^2_{sol} or Δm^2_{atm} are above or below their corresponding allowed values. This can help us select such a data set which has either of Δm^2_{sol} or Δm^2_{atm} inside the white region and the other one very near to its range. And then based on which mass squared difference is outside by what extent, one can determine how to bring in the fifth low scale parameter value inside its 3-σ range.

Consider figure 7a and figure 7b. In both the figures, for no values of $m_{lightest}(m_1)$, Δm^2s and $m_{\beta\beta}$ lie in their allowed ranges simultaneously. In conclusion, for this set of φ's, we can not have both Δm^2_{sol} and Δm^2_{atm} inside their 3-σ ranges satisfying the $m_{\beta\beta}$ constraint and thus we can discard this set of φ_1, φ_1 values. From figure 7c, we can see that there are only 3 combinations of φ_1 and φ_2 for which all three neutrino angles could be brought in. But again for allowed $m_{\beta\beta}$ values, there is no value of $m_{lightest}$ where both Δm^2_{sol} and Δm^2_{atm} can simultaneously lie within their 3-σ ranges. Thus this set of values can also be rejected The discussion for figure 7e and figure 7f is pretty much the same, except for the fact that there is only one pair of φ_1 and φ_2, out of the chosen ones, brings all angles inside. But again Δm^2_{sol}, Δm^2_{atm} and $m_{\beta\beta}$ cannot all be brought simultaneously within their allowed ranges for any choice of $m_{lightest}$.

Similarly, we have searched for many possible combinations of Majorana phases some of which are summarized in table 3 which shows whether or not the low scale parameters are within their 3-σ ranges for each pair of φ_1, φ_2 examined. From table 3, it is clear that with $m_{\beta\beta}$ constraint applied, we can not bring in Δm^2_{atm} and Δm^2_{sol}, along with all 3 angles, inside their allowed ranges simultaneously for any combination of high scale φ's. It is to be noted that in spite of examining only a few discrete values of φ's, we can claim this for the whole range $[0,2\pi]$ because Δm^2_{atm} varies monotonously and continuously with φ's.

Thus, we can conclude that although this case initially appeared to be promising; upon closer inspection we found that this case also doesn't lead to any viable parameter space where HSMU ansatz is compatible with the current experimental data. However, before completely rejecting the HSMU ansatz we need to perform one final check- namely the effect of SUSY threshold corrections on the low scale values of neutrino oscillation parameters, which we present in the next section.

5 Low energy SUSY threshold corrections

As we can see from table 3, for many sets of φ_1, φ_2; along with $m_{\beta\beta}$ we can bring in 4 out of 5 oscillation parameters inside their 3-σ ranges. One of the mass squared difference could not be brought inside its allowed range for any choice of the free parameters. However, in past works it was shown that certain SUSY threshold corrections can have impact on the low scale values of the neutrino oscillation parameters, in particular the values of the mass squared differences [9, 13]. The important threshold correction relevant to our analysis are given in appendix B.

JHEP07(2023)151

$\varphi_1(^\circ)$	$\varphi_2(^\circ)$	θ_{12}	θ_{13}	θ_{23}	Δm^2_{sol}	$\Delta m^2_{\rm atm}$
50	0	✓	✓	✓	✓	×
100	0	✓	✓	✓	×	×
200	0	✓	✓	✓	×	×
300	0	✓	×	✓	✓	×
0	50	✓	×	✓	✓	×
50	50	✓	×	✓	✓	×
100	50	✓	✓	✓	×	×
200	50	✓	×	✓	×	×
300	50	✓	✓	✓	✓	×
0	100	✓	×	✓	✓	×
50	100	✓	×	✓	✓	×
100	100	✓	✓	✓	×	×
200	100	✓	×	✓	×	×
300	100	✓	×	✓	✓	×
0	200	✓	×	×	×	×
50	200	✓	×	✓	✓	×
100	200	✓	×	✓	×	×
200	200	✓	×	✓	×	×
300	200	✓	✓	×	×	✓
0	300	✓	×	✓	✓	×
50	300	✓	✓	✓	✓	×
100	300	✓	✓	✓	×	×
200	300	✓	✓	✓	✓	×
300	300	✓	×	✓	✓	×

Table 3. '✓' represents that the corresponding parameter is within its experimental 3-σ range. $\mathrm{m}_{\beta\beta}$ is inside its bounds for ALL combinations of φ_1, φ_2. In some cases, we can bring one of the mass squared difference in at the expense of keeping $\mathrm{m}_{\beta\beta}$ outside its bound.

In order to see if inclusion of threshold corrections can lead to a viable parameter space consistent with current experimental data, we try to first see how that changes the lower values of $\Delta\mathrm{m}^2_{\rm atm}$ and $\Delta\mathrm{m}^2_{\rm sol}$. For this we choose one of the most promising pair of values of $\varphi_1 = 100^\circ$ and $\varphi_2 = 50^\circ$ from table 3, for which we were able to bring one mass squared difference inside its 3-σ range. After we add the threshold corrections large enough to bring the other mass squared difference inside its 3-σ range, we find that the other mass squared difference which was already inside its allowed range, now moves out of the experimental 3-σ range as shown in figures 8 and 9.

Figure 8 is plotted for the case when $\Delta\mathrm{m}^2_{\rm atm}$ is inside its 3-σ range without threshold corrections and $\Delta\mathrm{m}^2_{\rm sol}$ is outside. For this case we choose the masses of the s-particles such that the threshold corrections are large enough to bring $\Delta\mathrm{m}^2_{\rm sol}$ inside its 3-σ range, see eqs. (B.1)–(B.4) in appendix B. After adding the corrections with appropriate parameters

JHEP07(2023)151

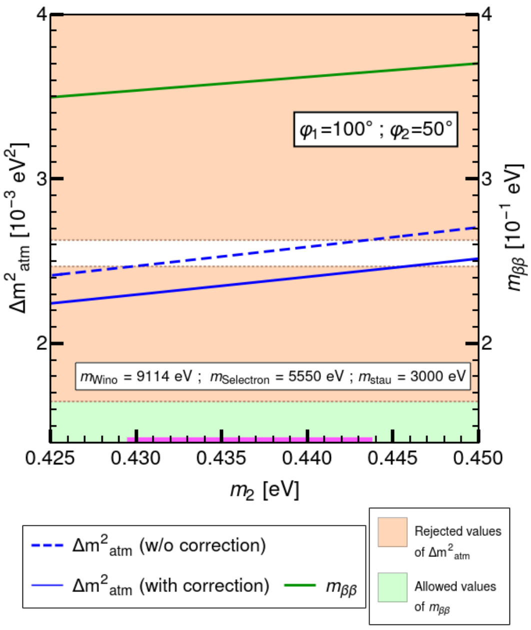

(a) Δm^2_{atm} and vs m_2.

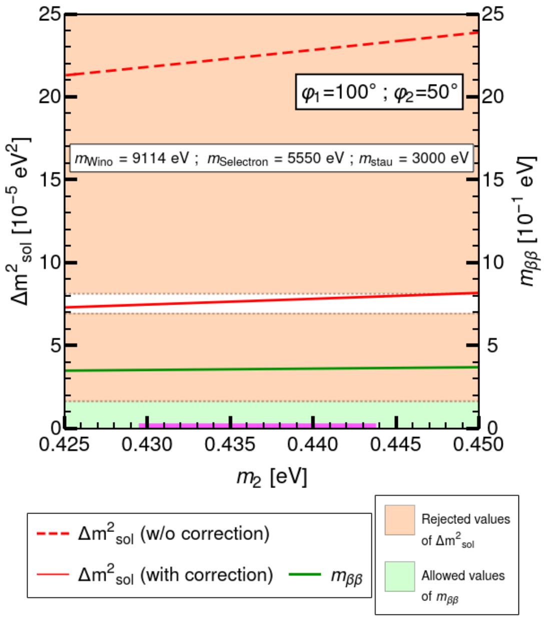

(b) Δm^2_{sol} and vs m_2.

Figure 8. Impact of threshold corrections on Δm^2_{atm} (left panel) and Δm^2_{sol} vs m_2 (right panel) with respect to m_2 mass eigen-state. The plots are done for the case where the uncorrected Δm^2_{atm} was inside its 3-σ range (white band) and Δm^2_{sol} is brought inside its allowed range after threshold corrections.

set, we find that the corrected Δm^2_{sol} can indeed be brought inside its 3-σ range, figure 8b. We plot this against one of the GUT scale masses- m_2. The corresponding threshold corrections will naturally be added in Δm^2_{atm} too. But for the same set of m_2 values for which corrected Δm^2_{sol} was brought in; the corrected Δm^2_{atm} is significantly far from its 3-σ range, figure 8a.

The same process is repeated in the figure 9; except now Δm^2_{sol} is inside and Δm^2_{atm} outside its range, before threshold corrections are added. Even in this case, for the same range of m_2 values the threshold corrected Δm^2_{sol} shifts outside its 3-σ range, figure 9a when the corrected Δm^2_{atm} is successfully brought in its respective 3-σ range, figure 9b.

Thus in summary we have systematically analyzed all possible cases of HSMU ansatz, both for Dirac and Majorana neutrinos. Overall, we can conclude that HSMU ansatz is in conflict with the current 3-σ allowed global fit ranges for neutrinos oscillation parameters and constraints from $0\nu\beta\beta$ decays in case of Majorana neutrinos. Today's narrow 3-σ experimental ranges of neutrino oscillation parameters do not allow HSMU hypothesis to be a plausible unification idea. In the next segment of the paper we discuss about an ansatz which generalizes the HSMU ansatz by imposing a looser set of demands on the high scale structure of the leptonic mixing matrix.

6 Wolfenstein ansatz

It was evident from previous sections that in no case the HSMU ansatz's prediction for all low scale neutrino parameters is consistent with their current 3-σ ranges. For this reason,

JHEP07(2023)151

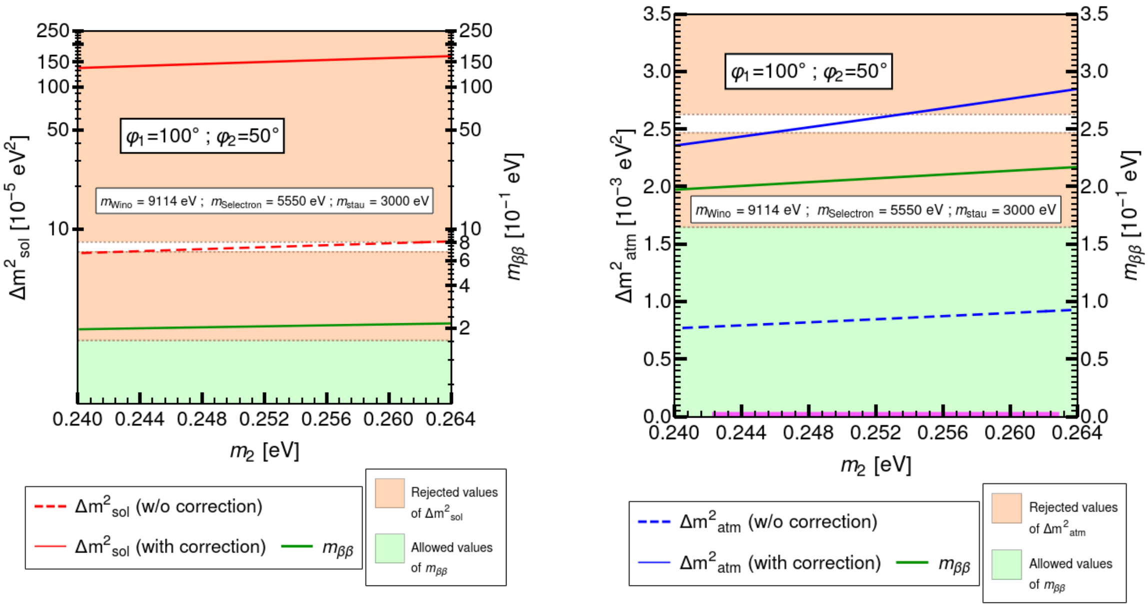

(a) Δm^2_{sol} and vs m_2.

(b) Δm^2_{atm} and vs m_2.

Figure 9. Impact of threshold corrections on Δm^2_{atm} (left panel) and Δm^2_{sol} vs m_2 (right panel) with respect to m_2 mass eigen state. This figure assumes that the uncorrected Δm^2_{sol} is inside its range (white band) and Δm^2_{atm} is brought inside its allowed range after threshold corrections.

we will like to consider another ansatz which tries to explain the hierarchical nature of neutrino mixing angles [16–19]. This ansatz lifts the stringent restrictions on high scale leptonic mixing angles put by HSMU. In HSMU we consider that the leptonic mixing angles are exactly equal to those of quarks at the high scale (GUT scale). But instead, here we consider that the hierarchy in high scale quark mixing angle is duplicated in leptonic angles as well. This hierarchy is parameterized by "Wolfenstein-like" form. In this case the leptonic mixing angles are in the following pattern

$$\sin\theta_{12} = \lambda \qquad \sin\theta_{23} = \lambda^2 \qquad \sin\theta_{23} = \lambda^3 \tag{6.1}$$

where λ is the leptonic Wolfenstein parameter which we define as the sine of the θ_{12} mixing angle. Wolfenstein parameter gives the neutrino mixing angles the following hierarchical structure-

$$\theta_{12} = \arcsin(\lambda) \qquad \theta_{23} = \arcsin(\lambda^2) \qquad \theta_{23} = \arcsin(\lambda^3) \tag{6.2}$$

We can vary θ_{23} and θ_{13} more finely by introducing α and β such that $\alpha, \beta > 0$, eq. (6.2) gets modified into

$$\theta_{12} = \arcsin(\lambda) \qquad \theta_{23} = \alpha \arcsin(\lambda^2) \qquad \theta_{13} = \beta \arcsin(\lambda^3) \tag{6.3}$$

Note that, choosing λ to be equal to 0.22532, α to be equal to 0.698353 and β to be equal to 0.264066 we get back the HSMU ansatz.

Since from HSMU ansatz we already saw that only the case of Majorana neutrinos (with non-zero values of φ_1, φ_2) is close to being viable, therefore for Wolfenstein ansatz we will limit ourselves to this case only. We will follow the same strategy already discussed for HSMU but now with the relaxed condition of Wolfenstein ansatz on the high scale leptonic mixing angles. For the initial study of Wolfenstein ansatz, we analyze the effects of varying α and β keeping Majorana phases to be zero and λ equal to the value corresponding to the HSMU ansatz($\lambda_{\rm HSMU} = 0.22532$). Once we find a suitable pair of α, β, we can study variations in λ. Only after thoroughly analyzing effects of α, β and λ we will bring in non-zero Majorana phases into the picture. The CP phase δ is taken to be equal to that of quarks CP violation phase($\delta_{\rm q}$) in all the cases.

6.1 Variations of α and β

Changing α and β can change the hierarchy of the angles at high scale which can possibly alter the usual RG running of the angles. Hence, to study variations of α, β we first analyze how the angles RG evolve for each pair of α, β we choose.

To obtain the graphs in figure 10 neutrino masses at high scales are chosen such that θ_{12} and θ_{13} are at their best fit value at low scale and θ_{23} at low scale is allowed to vary. The trend across the graphs shows that as α increases the span of θ_{23} shrinks and shifts higher in values. As a result of this, for a particular value of α, only for a few β values, all three angles have values within their experimental 3-σ range. For example from figure 10d and figure 10e it can be seen that the entire span of θ_{23} lies outside of its allowed range, i.e. for $\alpha = 0.8$ and $\alpha = 1.0$, we can not have all three mixing angles inside their allowed ranges.

6.2 Variation of λ

Having understood how different values of α, β are changing the RG evolution of the mixing angles, let us now see how variation in λ values changes it. Out of 25 pairs of α, β analyzed in previous section we choose the 20 valid pairs for which we analyze low scale values of θ_{12}, θ_{23}, θ_{13}, $\Delta m^2_{\rm sol}$, $\Delta m^2_{\rm atm}$ as well as $m_{\beta\beta}$. Note that we have still kept the Majorana phases to be zero. Its effects are to be seen later.

Figure 11 shows the impact of variation of λ on all the low scale mixing parameters as well as $m_{\beta\beta}$. We use high scale neutrino masses (free parameters) such that θ_{12}, θ_{13} and $\Delta m^2_{\rm sol}$ are fixed at their best fit values. Since, all the parameters are correlated, the RG evolution of θ_{23}, $\Delta m^2_{\rm atm}$ and $m_{\beta\beta}$ is allowed to vary freely dictated the by the RG equations.

As we can see θ_{23} and $m_{\beta\beta}$ values decrease for increasing λ. While doing so, they cross their allowed range. The range of λ values where for some choice of other free parameters, at least one λ value leads to either θ_{23} or $m_{\beta\beta}$ inside its allowed range, is highlighted on X-axis of figure 11 by yellow color. For a specific pair of α and β we can compare these minimum values of λ above which all angles and $m_{\beta\beta}$ can be brought inside their respective 3-σ ranges. For example, in $\alpha = 0.2$ case, the λ-space for which all angles are inside allowed ranges does not overlap with λ-space for which $m_{\beta\beta}$ is inside its 3-σ range. Therefore, that case is omitted in figure 11. Although, note that even for $\alpha = 0.2$, we can still bring four out of the six parameters inside their allowed ranges, which is still an improvement over the HSMU case, where we could not even bring all three angles inside their range. This is an indication that Wolfenstein ansatz can potentially be more promising.

For next set of α values shown in figure 11, the results are even more promising. We can find an overlap between λ -spaces of angles (left panels) and $m_{\beta\beta}$ (right panels) for

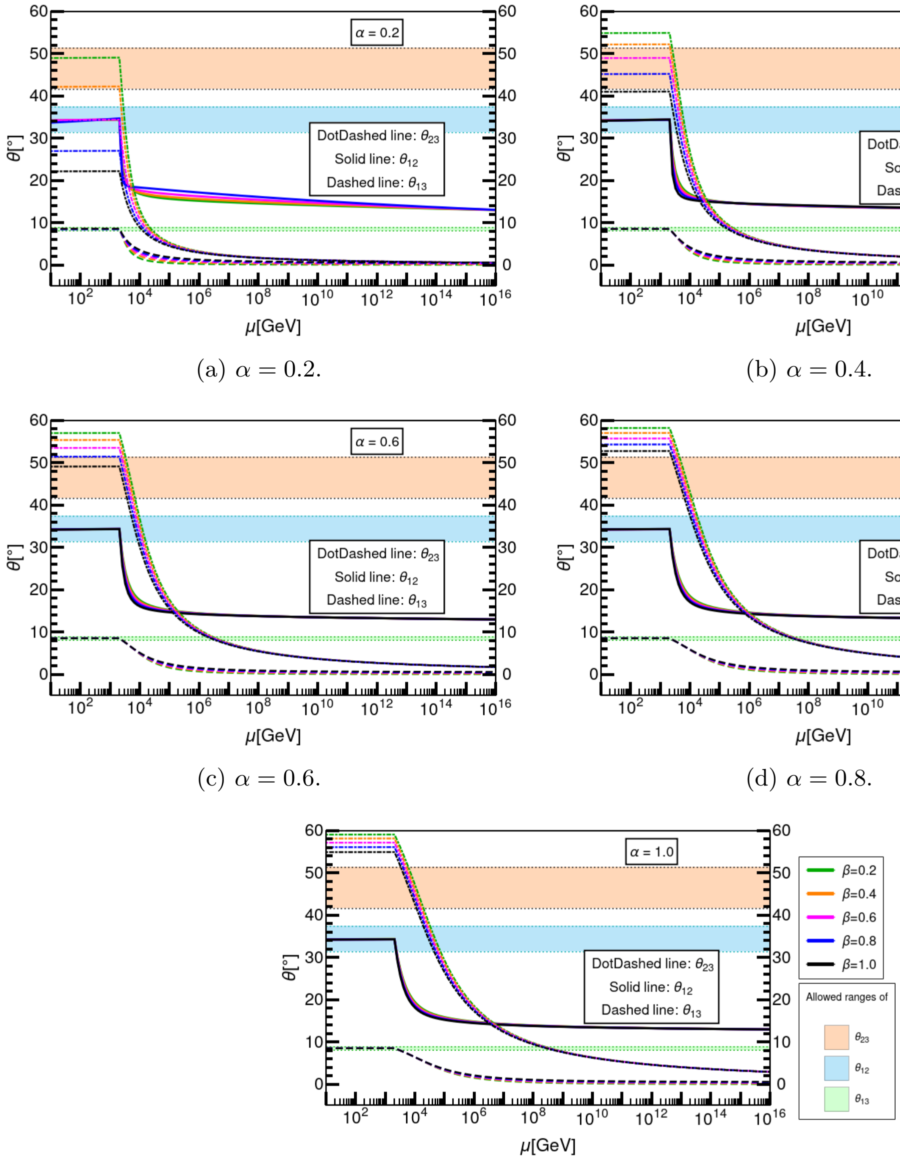

(a) $\alpha = 0.2$. (b) $\alpha = 0.4$.

(c) $\alpha = 0.6$. (d) $\alpha = 0.8$.

(e) $\alpha = 1.0$.

Figure 10. The RG evolution of neutrino mixing angles for various α, β pairs. Value of α is kept fixed for every graph and β is varied, represented by different colours. The shaded regions show 3-σ ranges for all three angles. For all the graphs $\lambda = \lambda_{\text{HSMU}} = 0.22532$.

same α. It means that for those λ values, we can bring in all angles, Δm^2_{sol} as well as $m_{\beta\beta}$ inside their 3-σ ranges, i.e., five out of six parameters but never all six simultaneously. Thus we have to investigate further by taking non-zero values of the Majorana phases (φ_1, φ_2) and study its effects on all the low scale parameters and see if all six can be brought inside.

6.3 φ_1, φ_2 variations

Here we will not span the entire φ_1, φ_2 space unnecessarily as it is computationally very expensive. In any case, the final goal is to find a set of input parameters for which all

JHEP07(2023)151

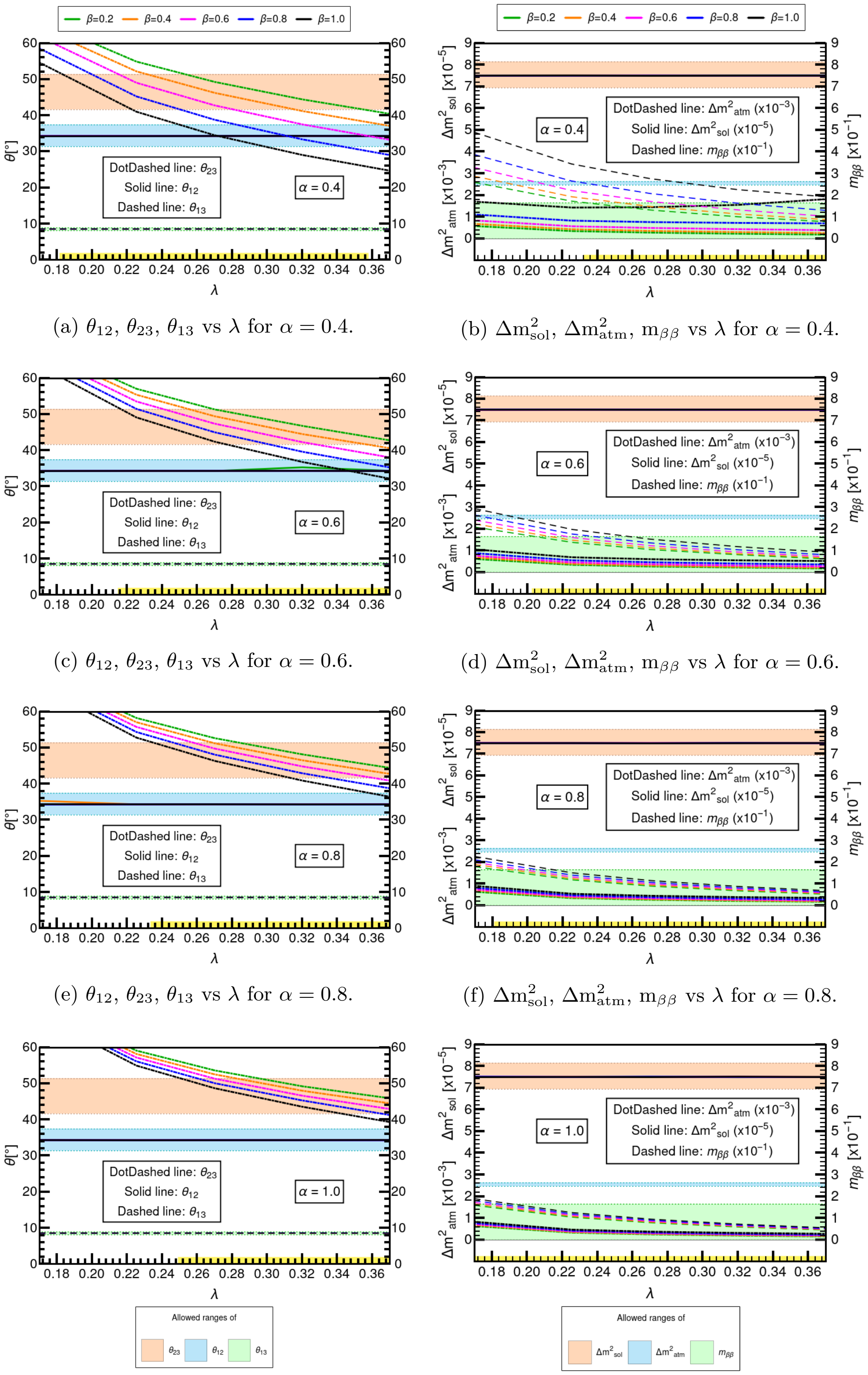

(a) θ_{12}, θ_{23}, θ_{13} vs λ for $\alpha = 0.4$.

(b) $\Delta m^2_{\rm sol}$, $\Delta m^2_{\rm atm}$, $m_{\beta\beta}$ vs λ for $\alpha = 0.4$.

(c) θ_{12}, θ_{23}, θ_{13} vs λ for $\alpha = 0.6$.

(d) $\Delta m^2_{\rm sol}$, $\Delta m^2_{\rm atm}$, $m_{\beta\beta}$ vs λ for $\alpha = 0.6$.

(e) θ_{12}, θ_{23}, θ_{13} vs λ for $\alpha = 0.8$.

(f) $\Delta m^2_{\rm sol}$, $\Delta m^2_{\rm atm}$, $m_{\beta\beta}$ vs λ for $\alpha = 0.8$.

(g) θ_{12}, θ_{23}, θ_{13} vs λ for $\alpha = 1.0$.

(h) $\Delta m^2_{\rm sol}$, $\Delta m^2_{\rm atm}$, $m_{\beta\beta}$ vs λ for $\alpha = 1.0$.

Figure 11. Impact of the variation of λ on all the low scale parameters. For each graph, value of α is kept fixed and β is varied. The shaded regions show 3-σ ranges for all three angles, mass squared differences and $m_{\beta\beta}$. See text for more details.

six parameters (angles, mass squared differences, $m_{\beta\beta}$) are inside their 3-σ ranges at low scale. We focus on the parameters which are set free to vary, i.e., θ_{23}, $\Delta m^2_{\rm atm}$ and $m_{\beta\beta}$. This is because other parameters are held constant at their best fit values using the three independent parameters namely the high scale neutrino masses. Thus, the newly introduced parameters λ, α and β along with Majorana phases can be scanned to find possible ranges where the low scale values of θ_{23}, $\Delta m^2_{\rm atm}$ and $m_{\beta\beta}$ are within their 3-σ range.

To have a simple and convenient start, we use the HSMU case to pick up only those φ_1, φ_2 pairs for which we could bring in all angles and one of the mass squared differences inside allowed ranges. In table 3, we list the values of φ_1, φ_2 where four oscillation parameters can be brought inside their 3-σ range.

$\varphi_1(^\circ)$	$\varphi_2(^\circ)$	θ_{12}	θ_{13}	θ_{23}	Δm^2_{sol}	$\Delta m^2_{\rm atm}$
50	0	✓	✓	✓	Only one	
50	300	✓	✓	✓	Only one	
200	300	✓	✓	✓	Only one	
300	50	✓	✓	✓	Only one	

For these values, we then discretely vary α and β. From α, β and λ variations shown in figure 11, it is observed that as λ increases, θ_{23}, $\Delta m^2_{\rm atm}$ and $m_{\beta\beta}$ decrease and vice versa. An exception to this trend is observed at lower values of α, where $\Delta m^2_{\rm atm}$ behaves the opposite for larger values of λ. One more reason to ignore low α values is that the span of θ_{23} is larger than its 3-σ range. Because of this, all β values for $\alpha = 0.2$ and $\alpha = 0.4$ should be discarded as for these values one can not bring θ_{23} value inside its 3-σ range.

Keeping this in mind, we ignore the lower α values here. For now, we shall only vary λ for those pairs of φ_1, φ_2 for which θ_{23}, $\Delta m^2_{\rm atm}$ and $m_{\beta\beta}$ are all either above/below their 3-σ ranges simultaneously or are all inside their 3-σ ranges simultaneously. This is because if one of the parameters from θ_{23}, $\Delta m^2_{\rm atm}$ and $m_{\beta\beta}$ lies on one side(higher or lower) of its own 3-σ range and other parameter lies on the opposite side of its own 3-σ range, changing λ will result in shifting one of the parameters away from its 3-σ range and thus not letting us bring in all the six low scale parameters in their allowed experimental bounds. This plan is case-wise realised in the following sub-section.

6.4 α, β, λ, φ_1, φ_2 variations combined

Now we shall choose the aforementioned φ_1, φ_2 pairs for α, β variation and select only those values for λ variations, for which θ_{23}, $\Delta m^2_{\rm atm}$ and $m_{\beta\beta}$ lie on one side of their respective 3-σ range. To illustrate this, a symbolic notation is used in order to understand the increasing/decreasing trend of these parameters.

Using various colours and shapes, tables 4 and 5 illustrate whether the respective parameter is inside, above or below the respective 3-σ ranges for various pairs of α, β and φ_1, φ_2. As discussed above, we ignore the lower values of α (0.4 and 0.2) as the λ variations don't assure either monotonic increase or monotonic decrease in $\Delta m^2_{\rm atm}$, for these α values. So in the rest, we want to get rid of those α, β pairs for which any two low scale parameters lie on opposite sides of their respective 3-σ ranges. In the symbolic representation, this translates to ruling out those data sets which have both green and red coloured symbols for the same α, β pairs. Let's consider the four cases one by one.

JHEP07(2023)151

α	β	θ_{23}	Δm^2_{atm}	$m_{\beta\beta}$
1.0	1.0	● (black)	● (red)	● (green)
1.0	0.8	⋆ (black)	● (red)	⋆ (green)
1.0	0.6	⋆ (green)	● (red)	● (black)
1.0	0.4	● (green)	● (red)	● (black)
1.0	0.2	● (green)	● (red)	● (black)
0.8	1.0	⋆ (red)	● (green)	● (green)
0.8	0.8	● (black)	● (red)	● (green)
0.8	0.6	⋆ (black)	● (red)	● (green)
0.8	0.4	⋆ (green)	● (red)	● (black)
0.8	0.2	● (green)	● (red)	● (black)
0.6	1.0	● (red)	● (green)	● (green)
0.6	0.8	⋆ (red)	● (green)	● (green)
0.6	0.6	● (black)	● (red)	● (green)
0.6	0.4	⋆ (black)	● (green)	● (green)
0.6	0.2	⋆ (green)	● (red)	● (black)
0.4	1.0	● (red)	● (red)	● (green)
0.4	0.8	● (red)	● (green)	● (green)
0.4	0.6	● (red)	● (green)	● (green)
0.4	0.4	⋆ (black)	● (red)	● (green)
0.4	0.2	⋆ (black)	● (red)	● (green)
0.2	1.0	● (red)	● (green)	● (green)
0.2	0.8	● (red)	● (green)	● (green)
0.2	0.6	● (red)	● (green)	● (green)
0.2	0.4	● (red)	● (green)	● (green)
0.2	0.2	⋆ (red)	● (red)	● (green)

(a) *For* $\varphi_1 = 50°$ *and* $\varphi_2 = 0°$.

α	β	θ_{23}	Δm^2_{atm}	$m_{\beta\beta}$
1.0	1.0	● (black)	● (red)	● (green)
1.0	0.8	⋆ (black)	● (red)	● (black)
1.0	0.6	⋆ (black)	● (red)	● (black)
1.0	0.4	⋆ (green)	● (red)	● (black)
1.0	0.2	⋆ (green)	● (red)	● (black)
0.8	1.0	⋆ (black)	● (green)	● (green)
0.8	0.8	● (black)	● (red)	● (green)
0.8	0.6	● (black)	● (red)	⋆ (green)
0.8	0.4	⋆ (black)	● (red)	● (black)
0.8	0.2	⋆ (green)	● (red)	● (black)
0.6	1.0	● (red)	● (red)	● (green)
0.6	0.8	⋆ (red)	● (green)	● (green)
0.6	0.6	● (black)	● (red)	● (green)
0.6	0.4	● (black)	● (red)	⋆ (green)
0.6	0.2	⋆ (black)	● (red)	⋆ (black)
0.4	1.0	● (red)	● (red)	● (green)
0.4	0.8	● (red)	● (red)	● (green)
0.4	0.6	● (red)	● (green)	● (green)
0.4	0.4	● (black)	● (red)	● (green)
0.4	0.2	● (black)	● (red)	● (green)
0.2	1.0	● (red)	● (red)	● (green)
0.2	0.8	● (red)	● (red)	● (green)
0.2	0.6	● (red)	● (red)	● (green)
0.2	0.4	● (red)	● (green)	● (green)
0.2	0.2	⋆ (black)	● (red)	● (green)

(b) *For* $\varphi_1 = 50°$ *and* $\varphi_2 = 300°$.

Table 4. The implications for the low scale values of θ_{23}, Δm^2_{atm} and $m_{\beta\beta}$ for various values of α and β for $\lambda = \lambda_{HSMU}$. The coloured symbols represent the following:
● (black): parameter value is inside 3-σ range
● (red): parameter value is below its lower bound
● (green): parameter value is above its upper bound
⋆ (black): parameter value is inside, but near the 3-σ boundary
⋆ (red): parameter value is *just* below its lower bound
⋆ (green): parameter value is *just* above its lower bound.

6.4.1 Case-1: $\varphi_1 = 50°$ and $\varphi_2 = 0°$

From the case when φ_1, φ_2 are 50° and 0° respectively, table 4a, we can see that red and green symbols occur together for every α, β pairs. Thus we can choose to ignore them for λ variations as it signifies that there exists at least one parameter among θ_{23}, Δm^2_{atm} and $m_{\beta\beta}$, which isn't inside its allowed 3-σ range. Since this happens for every α, β pair, it leaves us with no plausible sets of α, β pairs for λ variations. Thus we can rule out the Majorana phases pair $(50°, 0°)$ as a candidate to bring in all six low scale parameters.

6.4.2 Case-2: $\varphi_1 = 50°$ and $\varphi_2 = 300°$

For the case when φ_1, φ_2 are 50° and 300° respectively, from table 4b, we can see that every time red and green symbols occur together for the same α, β pairs we can choose to ignore them for λ variations as it signifies that there exists at least one parameter among θ_{23}, Δm^2_{atm} and $m_{\beta\beta}$, which does not come inside its allowed 3-σ range. This leaves us with only five plausible sets of α, β pairs. They are as follows:

α	1.0	1.0	0.8	0.8	0.6
β	0.8	0.6	1.0	0.4	0.2

In all these pairs, Δm^2_{atm} can be seen below its lower bound. In this set of α-β pairs some of them have low values α ($\alpha = 0.4, 0.2$). As discussed earlier, we ignore lower values of α because Δm^2_{atm} doesn't show monotonic increasing or monotonic decreasing trend for variations in λ. In the remaining α-β pairs, we will have to decrease λ in order to correct Δm^2_{atm}. But for all of these pairs of α-β, θ_{23} is given by '$\star$'; it represents that the values of θ_{23} are about to cross the upper bound of 3-σ range. Thus decreasing λ would increase the values of θ_{23} and it'll be out of its allowed range. Moreover, if we increase the value of λ it'll further decrease Δm^2_{atm} which is already below its allowed range. So, keeping both Δm^2_{atm} and θ_{23} inside their allowed ranges is not possible for any variation in λ. Thus we can, yet again, rule out the Majorana phases pair (300, 50) as a candidate to bring all six low scale parameters inside their respective 3-σ ranges.

6.4.3 Case-3: $\varphi_1 = 200°$ and $\varphi_2 = 300°$

From the case when φ_1, φ_2 are 200° and 300° respectively, we have the table 5a. We again choose to ignore simultaneous occurrences of red and green together for λ variations. This leaves us with only three plausible sets of α, β pairs. They are as follows

α	1.0	1.0	0.8
β	0.4	0.2	0.4

In all these pairs, Δm^2_{atm} is below its lower bound and in order to correct it, we will have to decrease λ such that Δm^2_{atm} increases. But note that for two of these pairs of α and β, θ_{23} is given by '$\star$', representing that θ_{23} is on the edge of its 3-σ range. Thus decreasing λ would shift θ_{23} immediately out of its allowed range and we won't be able to get θ_{23} inside when Δm^2_{atm} comes inside 3-σ range. Upon decreasing λ for the remaining case when $\alpha = 1.0$ and $\beta = 0.2$, the same argument applies even though θ_{23} value is inside 3-σ range. That is, it shifts θ_{23} again out of its allowed range and Δm^2_{atm} still doesn't come inside. This makes it impossible again to bring all six low scale parameters in. Thus we can again rule out the Majorana phases pair $(200°, 300°)$ as a candidate to bring in all six low scale parameters.

α	β	θ_{23}	Δm^2_{atm}	$m_{\beta\beta}$
1.0	1.0	$\color{green}{\bullet}$	$\color{red}{\bullet}$	$\bullet$
1.0	0.8	$\color{green}{\star}$	$\color{red}{\bullet}$	$\bullet$
1.0	0.6	$\color{green}{\star}$	$\color{red}{\bullet}$	$\bullet$
1.0	0.4	$\star$	$\color{red}{\bullet}$	$\bullet$
1.0	0.2	$\bullet$	$\color{red}{\bullet}$	$\bullet$
0.8	1.0	$\color{green}{\bullet}$	$\color{red}{\bullet}$	$\bullet$
0.8	0.8	$\color{green}{\bullet}$	$\color{red}{\bullet}$	$\bullet$
0.8	0.6	$\color{green}{\star}$	$\color{red}{\bullet}$	$\bullet$
0.8	0.4	$\star$	$\color{red}{\bullet}$	$\bullet$
0.8	0.2	$\bullet$	$\color{red}{\bullet}$	$\color{green}{\star}$
0.6	1.0	$\color{green}{\bullet}$	$\color{red}{\bullet}$	$\bullet$
0.6	0.8	$\color{green}{\bullet}$	$\color{red}{\bullet}$	$\bullet$
0.6	0.6	$\color{green}{\bullet}$	$\color{red}{\bullet}$	$\bullet$
0.6	0.4	$\color{green}{\star}$	$\color{red}{\bullet}$	$\bullet$
0.6	0.2	$\bullet$	$\color{red}{\bullet}$	$\color{green}{\bullet}$
0.4	1.0	$\color{green}{\bullet}$	$\color{red}{\bullet}$	$\bullet$
0.4	0.8	$\color{green}{\bullet}$	$\color{red}{\bullet}$	$\bullet$
0.4	0.6	$\color{green}{\bullet}$	$\color{red}{\bullet}$	$\bullet$
0.4	0.4	$\color{green}{\star}$	$\color{red}{\bullet}$	$\bullet$
0.4	0.2	$\star$	$\color{red}{\bullet}$	$\color{green}{\bullet}$
0.2	1.0	$\color{red}{\bullet}$	$\color{red}{\bullet}$	$\color{green}{\bullet}$
0.2	0.8	$\color{red}{\bullet}$	$\color{red}{\bullet}$	$\color{green}{\bullet}$
0.2	0.6	$\color{green}{\bullet}$	$\color{red}{\bullet}$	$\bullet$
0.2	0.4	$\color{green}{\bullet}$	$\color{red}{\bullet}$	$\bullet$
0.2	0.2	$\color{green}{\star}$	$\color{red}{\bullet}$	$\color{green}{\bullet}$

(a) *For* $\varphi_1 = 200^\circ$ *and* $\varphi_2 = 300^\circ$.

α	β	θ_{23}	Δm^2_{atm}	$m_{\beta\beta}$
1.0	1.0	$\star$	$\color{red}{\bullet}$	$\bullet$
1.0	0.8	$\color{green}{\star}$	$\color{red}{\bullet}$	$\bullet$
1.0	0.6	$\color{green}{\star}$	$\color{red}{\bullet}$	$\bullet$
1.0	0.4	$\color{green}{\star}$	$\color{red}{\bullet}$	$\bullet$
1.0	0.2	$\color{green}{\star}$	$\color{red}{\bullet}$	$\bullet$
0.8	1.0	$\star$	$\color{red}{\bullet}$	$\bullet$
0.8	0.8	$\star$	$\color{red}{\bullet}$	$\bullet$
0.8	0.6	$\color{green}{\star}$	$\color{red}{\bullet}$	$\bullet$
0.8	0.4	$\color{green}{\star}$	$\color{red}{\bullet}$	$\bullet$
0.8	0.2	$\color{green}{\star}$	$\color{red}{\bullet}$	$\bullet$
0.6	1.0	$\star$	$\color{red}{\bullet}$	$\bullet$
0.6	0.8	$\star$	$\color{red}{\bullet}$	$\bullet$
0.6	0.6	$\star$	$\color{red}{\bullet}$	$\bullet$
0.6	0.4	$\star$	$\color{red}{\bullet}$	$\bullet$
0.6	0.2	$\color{green}{\star}$	$\color{red}{\bullet}$	$\bullet$
0.4	1.0	$\star$	$\color{red}{\bullet}$	$\bullet$
0.4	0.8	$\star$	$\color{red}{\bullet}$	$\bullet$
0.4	0.6	$\star$	$\color{red}{\bullet}$	$\bullet$
0.4	0.4	$\star$	$\color{red}{\bullet}$	$\bullet$
0.4	0.2	$\star$	$\color{red}{\bullet}$	$\bullet$
0.2	1.0	$\star$	$\color{red}{\bullet}$	$\star$
0.2	0.8	$\star$	$\color{red}{\bullet}$	$\color{green}{\bullet}$
0.2	0.6	$\star$	$\color{red}{\bullet}$	$\color{green}{\bullet}$
0.2	0.4	$\star$	$\color{red}{\bullet}$	$\color{green}{\bullet}$
0.2	0.2	$\star$	$\color{red}{\bullet}$	$\color{green}{\bullet}$

(b) *For* $\varphi_1 = 300^\circ$ *and* $\varphi_2 = 50^\circ$.

Table 5. The implications for the low scale values of θ_{23}, Δm^2_{atm} and $m_{\beta\beta}$ for various values of α and β for $\lambda = \lambda_{HSMU}$. The coloured symbols represent the following:
$\bullet$: parameter value is inside 3-σ range
$\color{red}{\bullet}$: parameter value is below its lower bound
$\color{green}{\bullet}$: parameter value is above its upper bound
$\star$: parameter value is inside, but near the 3-σ boundary
$\color{red}{\star}$: parameter value is *just* below its lower bound
$\color{green}{\star}$: parameter value is *just* above its lower bound.

6.4.4 Case-4: $\varphi_1 = 300^\circ$ and $\varphi_2 = 50^\circ$

From the case when φ_1, φ_2 are 300° and 50° respectively, shown in table 5b, we again choose to ignore simultaneous occurrences of red and green together for λ variations. This time it leaves us with few more possibilities. It gives us total 13 plausible sets of α, β pairs

JHEP07(2023)151

for which we can then look for λ variations. They are as follows

α	1.0	0.8	0.8	0.6	0.6	0.6	0.6	0.4	0.4	0.4	0.4	0.4	0.2
β	1.0	1.0	0.8	1.0	0.8	0.6	0.4	1.0	0.8	0.6	0.4	0.2	1.0

In all these pairs, $\Delta m^2_{\rm atm}$ is below its lower bound. In this set of α-β pairs some of them have low values α ($\alpha = 0.4$, 0.2). As discussed earlier, we had already rejected lower values of α because $\Delta m^2_{\rm atm}$ doesn't show a monotonic increasing or a monotonic decreasing trend with variations in λ. In the remaining α-β pairs, we will have to decrease λ in order to correct $\Delta m^2_{\rm atm}$. But for all of these pairs of α-β, θ_{23} is given by '$\star$'; it represents that the values of θ_{23} are about to cross the upper bound of 3-σ range. Thus decreasing λ would increase the values of θ_{23} and they will be out of their allowed range. Moreover, if we increase the value of λ it will further decrease $\Delta m^2_{\rm atm}$ which is already below its allowed range. So, keeping both $\Delta m^2_{\rm atm}$ and θ_{23} inside their allowed ranges is not possible for any variation in λ. Thus we can, yet again, rule out the Majorana phases pair (300°, 50°) as here too one cannot bring all six low scale parameters inside their respective 3-σ ranges. Thus, to conclude, the leptonic mixing angles cannot have a Wolfenstein like hierarchical structure at high scale, as the resulting low scale values of the oscillation parameters and $m_{\beta\beta}$ are incompatible with their allowed experimental ranges.

7 Conclusions

The High Scale Mixing Unification ansatz was one of the appealing possibilities to understand the deeper connection between lepton and quark sectors. The ansatz implies that at some high energy scale, usually taken as the GUT scale, the quark and leptonic mixing matrices are unified. The apparent differences between the two mixing matrices at the low scale of the experiments is then attributed to the large change in the leptonic mixing angles due to RG evolution from the high to the low scale. Such large RG evolution can be achieved in SuperSymmetric models like MSSM with the SUSY breaking scale in the few TeV range. Since the leptonic mixing angles and the neutrino mass squared differences (observed in neutrino oscillations) RG evolve in a correlated fashion, this makes HSMU ansatz quite predictive. One of its early prediction was that θ_{13} angle should be non-zero but small [8], a fact later on confirmed by the experiments. In addition correlation between low scale values of θ_{13} and θ_{23} were also predicted [12, 13]. A generalization of the HSMU ansatz we call the Wolfenstein ansatz was also proposed in literature, where the strict requirement that at high scale the leptonic and quark mixing matrices are exactly same was relaxed. Instead the ansatz requires that the leptonic mixing angles at high scale should also have a hierarchical form, qualitatively similar to the one observed in the quark sector.

In this work we have thoroughly investigated both the HSMU and Wolfenstein ansatz, looking at the possibility of their compatibility with the current global fit results. We first started with the more stringent HSMU ansatz and investigated the various possibilities for both Dirac and Majorana neutrinos. For Dirac neutrinos we looked at the possibility of no CP violation as well as the possibility of CP violation in the leptonic sector. In both cases we found that for Dirac neutrinos, the current experimental data is completely incompatible

JHEP07(2023)151

with the HSMU hypothesis. We then looked at the Majorana cases, again looking at the possibility of zero and non-zero Majorana phases. For the case of zero Majorana phases, the results are similar to the Dirac case and is completely incompatible with current global fit results for the neutrino mixing angles. The case of non-zero Majorana phases was analysed in details and although we were able to have four of the neutrino oscillation parameters inside their current 3-σ range but we found that all the five oscillation parameters and $m_{\beta\beta}$ can never be simultaneously brought inside their allowed values, even after taking into account the SUSY threshold corrections. Thus we concluded that although promising in past, the HSMU hypothesis is no longer compatible with the current global fit results. Finally, we analyzed the various possibilities for the Wolfenstein ansatz and again we found that all the six observables (the five neutrino oscillation ones + $m_{\beta\beta}$) cannot be brought simultaneously inside their currently allowed ranges, for any choice of the free parameters. Thus, we conclude that the possibility of the leptonic mixing matrix having a hierarchical quark like form at a high scale is no longer viable.

Finally, note that throughout this work we have assumed the SM until it is supersymmetrized to MSSM at a higher scale, but this need not be the case. For example, the $\mathrm{SU}(2)_L \times \mathrm{U}(1)_Y$ gauge group of the SM can be replaced first by the Left-Right symmetric electroweak theory after a threshold and at a still higher threshold SUSY can come. It is worthwhile to see whether such modifications can bring the neutrino parameters to agree with the experimental data. Since the current analysis shows that the hypothesis is still very close to the experimentally allowed range, it is most likely that such modifications can bring exact agreement. This will be done in future work.

Acknowledgments

This work is dedicated to our mentor and collaborator Prof. G. Rajasekaran whose unwavering enthusiasm was instrumental in the successful completion of this work. Sadly Prof. Rajasekaran passed away while the manuscript was under review. The work of RS was supported by the SERB, Government of India grant SRG/2020/002303.

A Input parameters in bottom-up and top-down RG runnings

- $\mathrm{M_Z}$ scale = 91.1876 GeV
- GUT scale = 2×10^{16} GeV
- tanβ = 55 (β is the ratio of expectation values of Higgs doublets in 2HDM)
- SUSY cutoff scale = 2000 GeV
- Values of gauge coupling constants
    - Higgs coupling = 0.4615 (at $\mathrm{M_Z}$ scale) & 0.7013 (at GUT scale)
    - Weak coupling = 0.6519 (at $\mathrm{M_Z}$ scale) & 0.6904 (at GUT scale)
    - Strong coupling = 1.2198 (at $\mathrm{M_Z}$ scale) & 0.6928 (at GUT scale)

JHEP07(2023)151

- Quark mixing parameters at $\mathrm{M_Z}$ scale (mixing angles and Yukawa matrix elements) (Using table 1 and ref. [20])
- Lepton Yukawa matrix elements at $\mathrm{M_Z}$ scale (Using table 2 and refs. [20, 28])
- Quark and Lepton CP violation phases
- Self Higgs coupling $(\lambda) = 0.1291$
- Higgs ground state VEV$(\nu) = 246\,\mathrm{GeV}$

Values where sources are not mentioned are either computed using [26] or taken from [20].

B Dominant SUSY threshold corrections

To compute the low scale threshold corrections we will use the following parameters

$\Lambda =$ SUSY breaking scale

$\mathrm{g_{w,\Lambda}} = \mathrm{g_{cut}} =$ Weak coupling at SUSY breaking scale$(\Lambda) = 0.6354$

$\theta_{12,\Lambda} =$ Solar mixing angle at$\Lambda = 34.4153°$

$\varphi_{1,\Lambda}, \varphi_{2,\Lambda} =$ Majorana phases at $\Lambda = 15.5832°$ & $359.164°$

$\mathrm{m_{1,\Lambda}, m_{2,\Lambda}, m_{3,\Lambda}} =$ Neutrino masses at $\Lambda = 0.245775$ eV, 0.245973 eV & 0.248218 eV

We also define few functions which we need in threshold corrections formulae.

$\mathrm{p(x,y)} = \frac{\mathrm{x}}{\mathrm{y}}$

$\mathrm{q(x,y)} = 1 - \mathrm{p}^2$

$\mathrm{t(x,y)} = \frac{\mathrm{g_{cut}^2}}{32\pi^2}\left[\frac{\mathrm{p^2(\Lambda,y)-p^2(x,y)}}{\mathrm{q(\Lambda,y)q(x,y)}} + \frac{\mathrm{q^2(x,y)}-1}{\mathrm{q^2(x,y)}}\ln(\mathrm{p^2(x,y)}) - \frac{\mathrm{q^2(\Lambda,y)}-1}{\mathrm{q^2(\Lambda,y)}}\ln(\mathrm{p^2(\Lambda,y)})\right]$

$\mathrm{m_{com}} = \frac{1}{3}(\mathrm{m_1^2 + m_2^2 + m_3^2}) \times 10^{-9}$

Finally, with these input values and functions we can calculate corrections in both $\Delta\mathrm{m^2_{atm}}$ and $\Delta\mathrm{m^2_{sol}}$ as follows

$$(\Delta\mathrm{m^2_{sol}})_{\mathrm{corr}} = 4\mathrm{m^2_{com}}\Big[[\sin^2(\theta_{12,\Lambda})\cos(2\varphi_{2,\Lambda}) - \cos^2(\theta_{12,\Lambda})\cos(2\varphi_{1,\Lambda})]\times t(m_{\mathrm{selectron}}, m_{\mathrm{Wino}}) + [\cos^2(\theta_{12,\Lambda})\cos(2\varphi_{2,\Lambda}) - \sin^2(\theta_{12,\Lambda})\cos(2\varphi_{1,\Lambda})]\times t(m_\Lambda, m_{\mathrm{Wino}})\Big]\times 10^{18} \tag{B.1}$$

$$(\Delta\mathrm{m^2_{atm}})_{\mathrm{corr}} = 4\mathrm{m^2_{com}}\Big[-\cos^2(\theta_{12,\Lambda})\cos(2\varphi_{1,\Lambda})\times t(m_{\mathrm{selectron}}, m_{\mathrm{Wino}}) + [1-\sin^2(\theta_{12,\Lambda})\cos(2\varphi_{1,\Lambda})]\times t(m_\Lambda, m_{\mathrm{Wino}})\Big]\times 10^{18} \tag{B.2}$$

The corrected mass squared differences are given by

$$\Delta m^2_{sol} = (\Delta m^2_{sol})_{\mathrm{RG}} + (\Delta m^2_{sol})_{\mathrm{corr}} \tag{B.3}$$

$$\Delta m^2_{\mathrm{atm}} = (\Delta m^2_{\mathrm{atm}})_{\mathrm{RG}} + (\Delta m^2_{\mathrm{atm}})_{\mathrm{corr}} \tag{B.4}$$

JHEP07(2023)151

References

[1] ATLAS collaboration, *Observation of a new particle in the search for the Standard Model Higgs boson with the ATLAS detector at the LHC*, *Phys. Lett. B* **716** (2012) 1 [arXiv:1207.7214] [INSPIRE].

[2] CMS collaboration, *Observation of a New Boson at a Mass of* 125 *GeV with the CMS Experiment at the LHC*, *Phys. Lett. B* **716** (2012) 30 [arXiv:1207.7235] [INSPIRE].

[3] Super-Kamiokande collaboration, *Evidence for oscillation of atmospheric neutrinos*, *Phys. Rev. Lett.* **81** (1998) 1562 [hep-ex/9807003] [INSPIRE].

[4] SNO collaboration, *Direct evidence for neutrino flavor transformation from neutral current interactions in the Sudbury Neutrino Observatory*, *Phys. Rev. Lett.* **89** (2002) 011301 [nucl-ex/0204008] [INSPIRE].

[5] Daya Bay collaboration, *Observation of electron-antineutrino disappearance at Daya Bay*, *Phys. Rev. Lett.* **108** (2012) 171803 [arXiv:1203.1669] [INSPIRE].

[6] RENO collaboration, *Observation of Reactor Electron Antineutrino Disappearance in the RENO Experiment*, *Phys. Rev. Lett.* **108** (2012) 191802 [arXiv:1204.0626] [INSPIRE].

[7] Daya Bay collaboration, *Measurement of the Electron Antineutrino Oscillation with* 1958 *Days of Operation at Daya Bay*, *Phys. Rev. Lett.* **121** (2018) 241805 [arXiv:1809.02261] [INSPIRE].

[8] R.N. Mohapatra, M.K. Parida and G. Rajasekaran, *High scale mixing unification and large neutrino mixing angles*, *Phys. Rev. D* **69** (2004) 053007 [hep-ph/0301234] [INSPIRE].

[9] R.N. Mohapatra, M.K. Parida and G. Rajasekaran, *Threshold effects on quasi-degenerate neutrinos with high-scale mixing unification*, *Phys. Rev. D* **71** (2005) 057301 [hep-ph/0501275] [INSPIRE].

[10] R.N. Mohapatra, M.K. Parida and G. Rajasekaran, *Radiative magnification of neutrino mixings in split supersymmetry*, *Phys. Rev. D* **72** (2005) 013002 [hep-ph/0504236] [INSPIRE].

[11] S.K. Agarwalla, M.K. Parida, R.N. Mohapatra and G. Rajasekaran, *Neutrino Mixings and Leptonic CP Violation from CKM Matrix and Majorana Phases*, *Phys. Rev. D* **75** (2007) 033007 [hep-ph/0611225] [INSPIRE].

[12] G. Abbas, S. Gupta, G. Rajasekaran and R. Srivastava, *High Scale Mixing Unification for Dirac Neutrinos*, *Phys. Rev. D* **91** (2015) 111301 [arXiv:1312.7384] [INSPIRE].

[13] G. Abbas, S. Gupta, G. Rajasekaran and R. Srivastava, *Predictions from High Scale Mixing Unification Hypothesis*, *Phys. Rev. D* **89** (2014) 093009 [arXiv:1401.3399] [INSPIRE].

[14] R. Srivastava, *Predictions From High Scale Mixing Unification Hypothesis*, *Pramana* **86** (2016) 425 [arXiv:1503.07964] [INSPIRE].

[15] R. Srivastava, *High Scale Unification of CKM and PMNS Mixing Matrices*, *Springer Proc. Phys.* **174** (2016) 369 [INSPIRE].

[16] G. Abbas et al., *High scale mixing relations as a natural explanation for large neutrino mixing*, *Int. J. Mod. Phys. A* **31** (2016) 1650095 [arXiv:1506.02603] [INSPIRE].

[17] G. Abbas, M.Z. Abyaneh and R. Srivastava, *Precise predictions for Dirac neutrino mixing*, *Phys. Rev. D* **95** (2017) 075005 [arXiv:1609.03886] [INSPIRE].

[18] S.S. AbdusSalam, M.Z. Abyaneh, F. Ghelichkhani and M. Noormandipour, *Majorana phases in high-scale mixing unification hypotheses*, *Int. J. Mod. Phys. A* **36** (2021) 2150077 [arXiv:1912.13508] [INSPIRE].

[19] G. Rajasekaran, *Does the Wolfenstein form work for the leptonic mixing matrix?*, arXiv:1907.08380 [INSPIRE].

[20] Particle Data Group collaboration, *Review of Particle Physics*, *Phys. Rev. D* **98** (2018) 030001 [INSPIRE].

[21] J.A. Casas, J.R. Espinosa, A. Ibarra and I. Navarro, *General RG equations for physical neutrino parameters and their phenomenological implications*, *Nucl. Phys. B* **573** (2000) 652 [hep-ph/9910420] [INSPIRE].

[22] S. Antusch et al., *Neutrino mass operator renormalization revisited*, *Phys. Lett. B* **519** (2001) 238 [hep-ph/0108005] [INSPIRE].

[23] S. Antusch et al., *Neutrino mass operator renormalization in two Higgs doublet models and the MSSM*, *Phys. Lett. B* **525** (2002) 130 [hep-ph/0110366] [INSPIRE].

[24] S. Antusch, J. Kersten, M. Lindner and M. Ratz, *Neutrino mass matrix running for nondegenerate seesaw scales*, *Phys. Lett. B* **538** (2002) 87 [hep-ph/0203233] [INSPIRE].

[25] S. Antusch, J. Kersten, M. Lindner and M. Ratz, *Running neutrino masses, mixings and CP phases: Analytical results and phenomenological consequences*, *Nucl. Phys. B* **674** (2003) 401 [hep-ph/0305273] [INSPIRE].

[26] S. Antusch et al., *Running neutrino mass parameters in see-saw scenarios*, *JHEP* **03** (2005) 024 [hep-ph/0501272] [INSPIRE].

[27] M. Lindner, M. Ratz and M.A. Schmidt, *Renormalization group evolution of Dirac neutrino masses*, *JHEP* **09** (2005) 081 [hep-ph/0506280] [INSPIRE].

[28] P.F. de Salas et al., *2020 global reassessment of the neutrino oscillation picture*, *JHEP* **02** (2021) 071 [arXiv:2006.11237] [INSPIRE].

[29] E. Ma and R. Srivastava, *Dirac or inverse seesaw neutrino masses with $B-L$ gauge symmetry and S_3 flavor symmetry*, *Phys. Lett. B* **741** (2015) 217 [arXiv:1411.5042] [INSPIRE].

[30] E. Ma, N. Pollard, R. Srivastava and M. Zakeri, *Gauge $B-L$ Model with Residual Z_3 Symmetry*, *Phys. Lett. B* **750** (2015) 135 [arXiv:1507.03943] [INSPIRE].

[31] E. Ma and R. Srivastava, *Dirac or inverse seesaw neutrino masses from gauged $B-L$ symmetry*, *Mod. Phys. Lett. A* **30** (2015) 1530020 [arXiv:1504.00111] [INSPIRE].

[32] S. Centelles Chuliá, E. Ma, R. Srivastava and J.W.F. Valle, *Dirac Neutrinos and Dark Matter Stability from Lepton Quarticity*, *Phys. Lett. B* **767** (2017) 209 [arXiv:1606.04543] [INSPIRE].

[33] S. Centelles Chuliá, R. Srivastava and J.W.F. Valle, *Generalized Bottom-Tau unification, neutrino oscillations and dark matter: predictions from a lepton quarticity flavor approach*, *Phys. Lett. B* **773** (2017) 26 [arXiv:1706.00210] [INSPIRE].

[34] S. Centelles Chuliá, R. Srivastava and J.W.F. Valle, *Seesaw roadmap to neutrino mass and dark matter*, *Phys. Lett. B* **781** (2018) 122 [arXiv:1802.05722] [INSPIRE].

[35] S. Centelles Chuliá, R. Srivastava and J.W.F. Valle, *Seesaw Dirac neutrino mass through dimension-six operators*, *Phys. Rev. D* **98** (2018) 035009 [arXiv:1804.03181] [INSPIRE].

JHEP07(2023)151

[36] C. Bonilla et al., *Dark matter stability and Dirac neutrinos using only Standard Model symmetries*, *Phys. Rev. D* **101** (2020) 033011 [arXiv:1812.01599] [INSPIRE].

[37] S. Centelles Chuliá, R. Cepedello, E. Peinado and R. Srivastava, *Systematic classification of two loop $d = 4$ Dirac neutrino mass models and the Diracness-dark matter stability connection*, *JHEP* **10** (2019) 093 [arXiv:1907.08630] [INSPIRE].

[38] S. Centelles Chuliá, R. Srivastava and A. Vicente, *The inverse seesaw family: Dirac and Majorana*, *JHEP* **03** (2021) 248 [arXiv:2011.06609] [INSPIRE].

[39] S.C. Chuliá, *Theory and phenomenology of Dirac neutrinos*, arXiv:2110.15755 [INSPIRE].

[40] PLANCK collaboration, *Planck 2018 results. VI. Cosmological parameters*, *Astron. Astrophys.* **641** (2020) A6 [*Erratum ibid.* **652** (2021) C4] [arXiv:1807.06209] [INSPIRE].

[41] KATRIN collaboration, *Direct neutrino-mass measurement with sub-electronvolt sensitivity*, *Nature Phys.* **18** (2022) 160 [arXiv:2105.08533] [INSPIRE].

[42] S. Weinberg, *Baryon and Lepton Nonconserving Processes*, *Phys. Rev. Lett.* **43** (1979) 1566 [INSPIRE].

[43] KAMLAND-ZEN collaboration, *Search for Majorana Neutrinos near the Inverted Mass Hierarchy Region with KamLAND-Zen*, *Phys. Rev. Lett.* **117** (2016) 082503 [*Addendum ibid.* **117** (2016) 109903] [arXiv:1605.02889] [INSPIRE].

JHEP07(2023)151